

Initial Clinical Experience with a Radiation Oncology Dedicated Open 1.0T MR-Simulation

Carri K Glide-Hurst¹, Ning Wen¹, David Hearshen¹, Milan Pantelic¹, Bo Zhao¹, Yanle Hu², Tina Kunkel¹, Kenneth Levin¹, Benjamin Movsas¹, Indrin J. Chetty¹, and M. Salim Siddiqui¹

¹Henry Ford Health System, Detroit, MI, United States, ²Washington University, St Louis, MO, United States

Purpose: Due to its excellent soft tissue contrast, MRI is often integrated as an adjunct to computed tomography simulation (CT-SIM) for radiotherapy (RT) treatment planning to assist in tumor and organ at risk delineation. Recently, dedicated MR simulation (MR-SIM) platforms for radiation oncology have been introduced, although paucity in the literature exists on how to fully implement MR-SIM into the clinic. This work describes our initial experience with characterizing system performance, establishes quality assurance (QA) programs, and sets the context for dedicated MR-SIM for RT.

Methods: Characterization of a 1.0T Philips Panorama High Field Open (HFO) MRI (Philips Medical Systems) was conducted using integrated software (RT Oncology Configuration, v3.5.2). Patient workflow was optimized including immobilization devices, flat couch overlay devices, and use of an external laser positioning system (ELPS) with six Class II lasers for patient positioning and alignment to correlate external skin marks and MR images. Spatial and volumetric analyses were conducted between CT-SIM and MR-SIM using a phantom with known volumes. To evaluate system-level 3D distortion, a 40 cm × 40 cm × 40 cm phantom with known landmarks was scanned with MR-SIM (integrated coil, 3D T1 Fast-field echo (FFE), TE/TR= 3.83/9 msec, voxel size ≈ 0.938 × 0.938 × 1 mm³) and CT-SIM (2 mm axial slice thickness, 120 kVp, voxel size ≈ 0.68 × 0.68). To derive a 3D distortion map, B-spline deformable image registration was conducted between MR-SIM and CT-SIM using Velocity Advanced Imaging (VelocityAI, v2.6.2) that we previously benchmarked¹ using CT-SIM as the distortion-free model. Displacement vector fields (DVs) were exported and assessed in isocentric rings 5-20 cm from isocenter (Fig 1) with results summarized via displacement histograms. Temporal monitoring of ACR image quality metrics, ELPS impact on image quality, and system performance (i.e. magnetic field homogeneity and central frequency) was performed. Routine clinical MR-SIM is underway for pelvis, brain, and spine and amplitude-based 4D-MRI² has been implemented in a research platform.

Results: Over four months, ELPS QA yielded <2 mm deviation from laser scribes with couch motion and individual laser motions <1 mm. Image quality metrics were within ACR recommendations. Slice thickness accuracy yielded a full-width half maximum of 4.94 ± 0.03 mm (nominal slice width = 5 mm), and transmitter gain was stable (0.63 ± 0.01 dB, range: 0.62-0.64 dB). Little deviation was observed for low contrast detectability. Magnetic field inhomogeneity was <2ppm over a 31 cm diameter sphere. Close concordance was obtained between CT-SIM and MR-SIM volumes (<3% from expected, Fig 2(left)). The mean distance between known landmarks was 59.5 ± 0.0 mm and 59.5 ± 0.5 mm for CT-SIM and MR-SIM, respectively. Importantly, 3D distortion was <3mm for 96% of all voxels in a 10cm radius of isocenter (Fig 1). At 15-20 cm away from isocenter, ~24% of voxels deformed >3mm. ELPS laser interference was within the operating frequency band of the MR scanner and was characterized by line patterns in the datasets, with reductions of signal-to-noise ratio ranging from 4.6-12.6% for TE values of 50-150 msec.

Discussion: We have established clinical workflow and QA processes for MR-SIM. Image quality and mechanical tests were within accepted criteria. To guide our clinicians on expected geometrical accuracy due to image distortion, 3D distortion analysis was conducted and non-negligible displacements between MR-SIM and CT-SIM occurred >15 cm from isocenter, most notably in the anterior and posterior regions for the axial view. This suggests that distortion will impact regions near the patient periphery and would need to be accounted for in MR-SIM-only treatment planning. We expect the worst-case scenario results to occur for large phantoms without dedicated coils, but expect that lateral translation of the area requiring the highest geometric fidelity (i.e. tumor) toward isocenter will help mitigate this effect.

Conclusions: Through a series of mechanical and image quality characterization tests, we developed the routine QA procedures necessary to implement MR-SIM into RT planning. Future work will involve characterization of patient-specific susceptibility-related distortions, which will vary based on the type of anatomy being imaged. These artifacts are known to increase with B0 field strength, and at 1.0 T, are expected to be <1-2 mm for most sites not influenced by respiratory motion.

References: 1. N. Stanley, C. Glide-Hurst, J. Kim, J. Adams, S. Li, N. Wen, I. J. Chetty, and H. Zhong, "Using Patient-Specific Phantoms to Evaluate Deformable Image Registration Algorithms for Adaptive Radiation Therapy," Journal of Applied Clinical Medical Physics (2013).
2. Y. Hu, S. D. Caruthers, D. A. Low, P. J. Parikh, and S. Mutic, "Respiratory Amplitude Guided 4-Dimensional Magnetic Resonance Imaging," International Journal of Radiation Oncology*Biophysics*Physics **86**, 198-204 (2013).

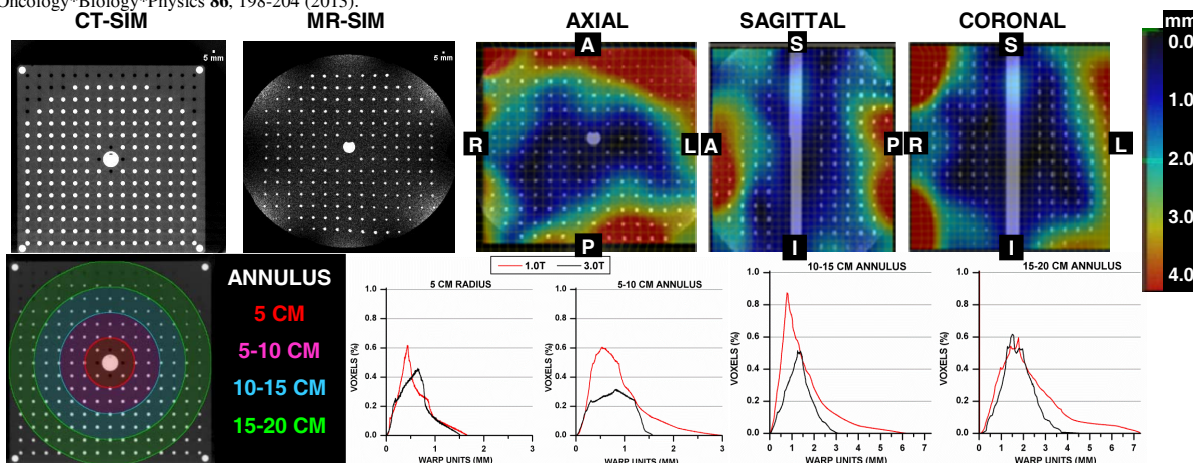


Fig 1: 3D distortion quantification. Top: 1.0T MR-SIM deformation maps to CT-SIM. Bottom: Region of interests and deformation results for distances from isocenter.

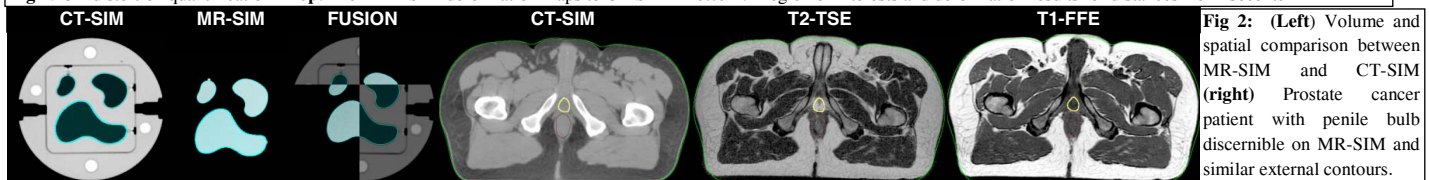


Fig 2: (Left) Volume and spatial comparison between MR-SIM and CT-SIM (right) Prostate cancer patient with penile bulb discernible on MR-SIM and similar external contours.